

## Nonmonotonic Friction due to Water Capillary Adhesion and Hydrogen Bonding at Multiasperity Interfaces

Liang Peng,<sup>1,\*</sup> Feng-Chun Hsia<sup>1,2</sup>, Sander Woutersen,<sup>1</sup> Mischa Bonn,<sup>1,3</sup> Bart Weber,<sup>1,2</sup> and Daniel Bonn<sup>1</sup>

<sup>1</sup>*Van der Waals-Zeeman Institute, Institute of Physics, University of Amsterdam, Science Park 904, 1098 XH Amsterdam, Netherlands*

<sup>2</sup>*Advanced Research Center for Nanolithography (ARCNL), Science Park 106, 1098 XG Amsterdam, Netherlands*

<sup>3</sup>*Molecular Spectroscopy Department, Max Planck Institute for Polymer Research, Ackermannweg 10, Mainz 55128, Germany*



(Received 30 May 2022; accepted 9 November 2022; published 16 December 2022)

Capillary adhesion due to water adsorption from the air can contribute to friction, especially for smooth interfaces in humid environments. We show that for multiasperity (naturally oxidized) Si-on-Si interfaces, the friction coefficient goes through a maximum as a function of relative humidity. An adhesion model based on the boundary element method that takes the roughness of the interfaces into account reproduces this nonmonotonic behavior very well. Remarkably, we find the dry friction to be significantly lower than the lubricated friction with macroscopic amounts of water present. The difference is attributed to the hydrogen-bonding network across the interface. Accordingly, the lubricated friction increases significantly if the water is replaced by heavy water ( $D_2O$ ) with stronger hydrogen bonding.

DOI: [10.1103/PhysRevLett.129.256101](https://doi.org/10.1103/PhysRevLett.129.256101)

The frictional properties of silicon-based materials have been of interest to researchers for several decades, given the importance of friction for technology development in the semiconductor industry, including, for instance, improving the efficiency and extending the lifetime of microelectromechanical systems [1–3]. Silicon components are often exposed to humid environments where capillary adhesion can occur across interfaces. This capillary adhesion is a key factor in increasing friction, especially for interfaces that are smooth compared with the range of the adhesive interaction [4,5]. Therefore, a fundamental understanding of how capillary adhesion and friction evolve with relative humidity, particularly at multiasperity systems, is essential to control friction and reduce wear from a technological perspective. Moreover, understanding how nanoscale adhesion and friction mechanisms manifest themselves at larger length scales remains a major scientific challenge.

Numerous experiments have been conducted to tackle challenges related to the increasing importance of capillary adhesion and friction in silicon systems. For hydrophilic (naturally oxidized) silicon, the humidity dependence of capillary adhesion and friction has been studied by atomic force microscopy (AFM) experiments: friction and adhesion first increase with increasing humidity and then decrease [6–8]. This nonmonotonic humidity dependence has been attributed to the competing roles of the Laplace pressure and the meniscus size at the interface; the former decreases with increasing relative humidity while the latter increases with increasing relative humidity [9–11]. Furthermore, the icelike structure of adsorbed water in humid conditions can strongly enhance nanoscale adhesion and friction at low humidities (below 40–80%) [3,6,12]. A similar nonmonotonic behavior has been observed for the adhesion of assemblies of sand

grains (with  $SiO_2$  surfaces similar to the silicon surfaces studied here) [13,14]. Here the nonmonotonic behavior was attributed to the roughness of the surfaces: before adhesive water bridges can form, the water first fills the small pores between the asperities of the surface [15].

Despite substantial theoretical efforts [11,16–18], few experiments [19,20] have addressed the mechanisms underlying the humidity dependence of capillary adhesion and its relation with friction at multiasperity interfaces. Two main complications exist. First, the direct measurement of the adhesive force is prohibited by the so-called adhesion paradox [21–23]: the elastic energy stored in asperities provides a repulsive force between the two surfaces that masks the adhesive force. Second, the friction experiments may induce wear, which, in turn, influences adhesion [4,5,24,25].

In this Letter, we experimentally show that multiasperity Si-on-Si friction increases with relative humidity in the range from 0 to 20% and decreases again when the relative humidity increases beyond 20%. The dependence of the friction at higher levels of relative humidity can be captured by a simple capillary adhesion model based on the boundary element method without adjustable parameters. With increasing relative humidity, the reduction in Laplace pressure, which controls the capillary adhesive force, drives the decrease of the friction coefficient. In addition, we find that the value of the friction coefficient for the completely dry case (no capillary bridges) is much lower than the completely immersed case, which also has no capillary bridges. We interpret the strong dependence of the friction on the relative humidity below 20% in terms of the hydrogen bonding across the interface, which is

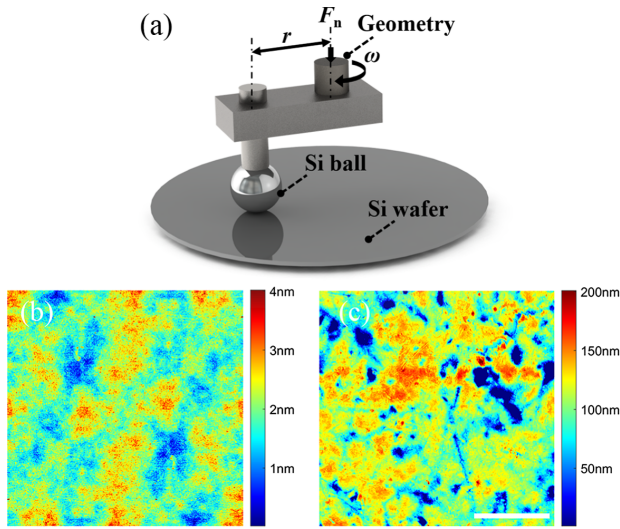


FIG. 1. Experimental setup (a). A silicon ball inside a humidity-controlled chamber is clamped to the geometry of a rheometer which is used to measure normal and frictional forces between the silicon ball and the silicon wafer. The known distance between the rotation axis and the sphere,  $r = 10$  mm, is used to translate the imposed rotation speed  $\omega$  into a sliding speed and to translate the imposed torque into a friction force. AFM images of the wafer (b) and silicon ball (c) are shown. The root-mean-squared roughness of the surfaces was 0.5 nm (wafer) and 40.5 nm (sphere), measured over an area of  $31.1331.13 \mu\text{m}^2$ . Scale bar, 10  $\mu\text{m}$ .

strongly reduced at humidities below 20%, but of course remains present for the completely immersed case.

Silicon-on-silicon friction experiments were performed with a rheometer (DSR 502, Anton Paar) inside a customized humidity-controlled chamber, as shown in Fig. 1. The partial pressure of water vapor or the relative humidity inside the chamber is controlled by a humidifier (MHG100, proUmid). Before the experiments, the silicon spheres were rinsed with ethanol and sonicated in Milli-Q water, followed by nitrogen flow drying. In the friction experiments, a clean, 3 mm-diameter rough silicon sphere was brought into contact with an as-received smooth *p*-doped silicon (100) wafer (University Wafer) with a native oxide layer. The surface chemistry during sliding may therefore be a complex mix of Si–Si, Si–SiO<sub>2</sub>, and SiO<sub>2</sub>–SiO<sub>2</sub>, due to the wear and reformation of the thin oxide layers on the silicon. The contact was formed under a normal load of 50 mN after the relative humidity inside the chamber was dried to 0.6%. The approximate contact diameter at 50 mN normal force was calculated to be 20  $\mu\text{m}$  based on the classical Hertzian contact theory. The sliding speed imposed by the rheometer was 100 nm/s in humidity-dependent experiments and varied from 0.1 to 100  $\mu\text{m}/\text{s}$  in the velocity-dependent experiments. During the sliding experiments, the rheometer moves the sphere tangentially on the wafer while measuring

both friction force ( $F_f$ ) and externally applied load ( $F_{\text{external}}$ ). The ratio of these two forces gives the friction coefficient (COF),  $\mu = F_f/F_{\text{external}}$ . It is important to note that any adhesion exerted at the interface is hidden in the sense that it may influence the measured friction force, but it does not contribute to the externally applied load. To minimize the influence of wear, sliding strokes were kept short at 3  $\mu\text{m}$  (as shown in Fig. S1 [26]), and each stroke was measured at a previously untouched section on the substrate. After a few strokes, the COF reached a steady state; we report the steady state values of the COF. The surface topography of the spheres was measured before and after friction experiments by laser-scanning confocal microscopy (Keyence VK-X1000) over an area of  $212293 \mu\text{m}^2$  (*XYZ* resolution of 400, 400, and 12 nm, respectively) to verify that only minimal wear occurred [4].

In the humidity-dependent friction experiments, we vary the relative humidity inside the chamber between 0.6 and 80%. The humidity is first increased and subsequently decreased again, in intervals of 20%. The COF is measured at each relative humidity. Before each change in the humidity, the chamber was first dried for 1 hour, by lowering the relative humidity to 0.6%, to remove any residual water. After drying, the system was equilibrated at the target humidity level for 1 hour before starting the friction measurement. During drying and equilibration, the sphere was kept in contact with the substrate. At the end of the humidity-dependent friction experiments, the contact was immersed in deionized water, and friction was measured. After all friction experiments were completed, the topography of the sphere apex within an area of  $31.1331.13 \mu\text{m}^2$  was captured by tapping mode AFM (Dimension Icon, Bruker) with Si tips (RTESPA-300, Bruker). Contact calculations using the AFM topography as input were carried out using the Tribology simulator [27].

To investigate the effect of interfacial bonding on friction, velocity-dependent experiments (0.1–100  $\mu\text{m}/\text{s}$ ) were conducted under dry and water-immersed conditions. Furthermore, the evolution of the COF in time was also measured while the contact was immersed in heavy water (D<sub>2</sub>O) instead of normal water (H<sub>2</sub>O). The heavy water was free to exchange with normal water in the surrounding 60% relative humidity environment.

As shown in Fig. 2, the friction coefficient evolves with relative humidity without any hysteresis, and can be divided into two regimes. In the first regime, the COF sharply increases when the relative humidity is increased from 0.6 to 20%. In the second regime, in which the relative humidity is between 20 and 80%, the friction decreases slightly with increasing relative humidity.

The observed nonmonotonic behavior is well captured by a simple adhesion model (solid green line in Fig. 2) which is detailed below. The adhesion model neglects the contribution of van der Waals forces to the adhesion, and

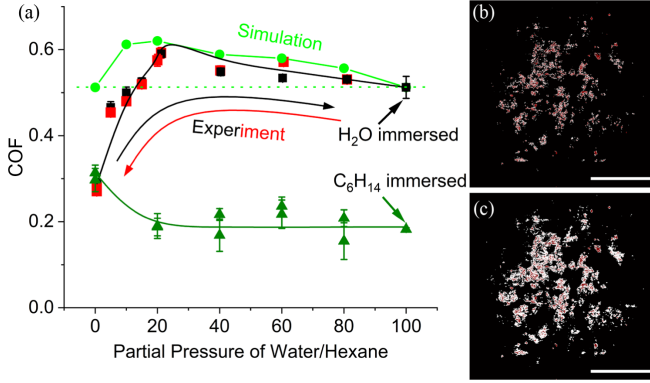


FIG. 2. Friction as a function of relative humidity (RH) and partial pressure of hexane (a). Measurements were performed with increasing (black squares) and decreasing (red squares) relative humidity to rule out significant hysteresis (more experiments are reported in Fig. S4 [26]). The corresponding simulation result is represented by the solid green circles. The olive triangles in (a) display the evolution of the friction coefficient with the partial pressure of hexane at a sliding velocity of 1  $\mu\text{m/s}$ . The hexane gas was introduced into the system after several sliding strokes were performed in the dry environment (leftmost data point). The relative humidity level for all hexane measurements was around 1%. Lines through the data points are drawn to guide the eye. (b) and (c) are two simulated contact maps under 20% RH (b) and 80% RH (c). The red, white, and black regions in the contact map correspond to the contact area, capillary area, and noncontact area without water bridges, respectively. Scale bar: 10  $\mu\text{m}$ .

only considers capillary adhesion [4,5]. As a result, the equilibrium of forces at the interface is given by Eq. (1).

$$\vec{F}_{\text{adhesion}} + \vec{F}_{\text{external}} + \vec{F}_{\text{elastic}} = 0 \quad (1)$$

where  $\vec{F}_{\text{adhesion}}$ ,  $\vec{F}_{\text{external}}$ , and  $\vec{F}_{\text{elastic}}$  are capillary adhesion, externally applied load, and elastic repulsive force, respectively. Multiasperity adhesion is hard to detect, as discussed above and shown in Fig. S3 [26]. To obtain a quantitative description, we employ a boundary element method contact calculations, in which the elastoplastic equations are discretized and solved numerically to solve the contact problem and estimate the capillary adhesion. Both the capillary adhesion and the elastic force are calculated as a function of the average interfacial gap. We assume that the locally experienced adhesion forces influence the average interfacial gap in the same way as an externally applied force does. The Tribology simulator can calculate the interface deformation associated with a given elastic repulsive force,  $F_{\text{elastic}}$ , using the measured surface topography and the mechanical properties of silicon (listed in Table S1). Subsequently, the adhesion force can be estimated based on the resulting interface geometry, which is described by the interfacial gap value as a function of the in plane position.

To estimate the capillary adhesion force in the calculations, it is assumed that water bridges form within regions called capillary areas, where the local interfacial gap is below a threshold value  $D$ . Within the capillary areas, there is capillary attraction due to the Laplace pressure difference between the inside and outside of the water bridges. The threshold value  $D$  is defined here as  $D = 2 \times H + D_c$ , in which  $H$  and  $D_c$  represent the absorbed water film thickness and the critical nucleation distance obtained from previous studies [6,28,29], as shown in Table S2. The capillary adhesive force,  $F_{\text{adhesion}}^{\text{simulated}}$ , is calculated by multiplying the Laplace pressure with the capillary area. The external load can then be obtained from Eq. (1).

To describe the influence of the capillary adhesion,  $\vec{F}_{\text{adhesion}}$ , on friction, we assume that the measured friction force,  $F_f$ , is proportional to the sum of the adhesion force,  $\vec{F}_{\text{adhesion}}$ , and the externally applied normal force,  $\vec{F}_{\text{external}}$ . This assumption is motivated by the observation of such load-controlled friction [30,31] in similar systems [5,32]. The proportionality constant that links the friction force to the combined normal force,  $|\vec{F}_{\text{adhesion}}| + |\vec{F}_{\text{external}}|$ , can be obtained by performing a water-immersed friction experiment in which there is no capillary adhesion, while the externally applied force and friction force can be measured. We thus obtain

$$\begin{aligned} \text{COF}_{\text{simulated}} &= \frac{\text{COF}_{\text{immersed}} \times |F_{\text{external}}| + \text{COF}_{\text{immersed}} \times |F_{\text{adhesion}}^{\text{simulated}}|}{|F_{\text{external}}|} \\ &= \text{COF}_{\text{immersed}} + \frac{|F_{\text{adhesion}}^{\text{simulated}}|}{|F_{\text{external}}|} \times \text{COF}_{\text{immersed}} \end{aligned} \quad (2)$$

in which the  $\text{COF}_{\text{simulated}}$  is the estimated friction coefficient in the adhesion model and  $\text{COF}_{\text{immersed}}$  is the friction coefficient measured when the system is immersed in water such that there is no capillary adhesion.

The match between the simulation result and the experimental result obtained in the 20–80% relative humidity regime shows that our proposed adhesion model, without adjustable parameters, is accurate. Capillary adhesion influences friction, and its impact depends on the superposition of two competing effects: growth of the capillary area and reduction of the Laplace pressure with increasing relative humidity. As the relative humidity increases, the range of the capillary adhesion, and thus the capillary area, increases due to the formation of thicker water layers [6] on the solid surfaces and due to the increased critical distance for capillary condensation, which scales with the (increasing) Kelvin radius [28]. The growing Kelvin radius, in turn, reduces the curvature of the liquid-gas interface, thereby reducing the Laplace pressure [6]. The nonmonotonic change in friction as a function of relative humidity is analogous to the change in shear modulus of sand with water content [13,14]: a small amount of water enhances the

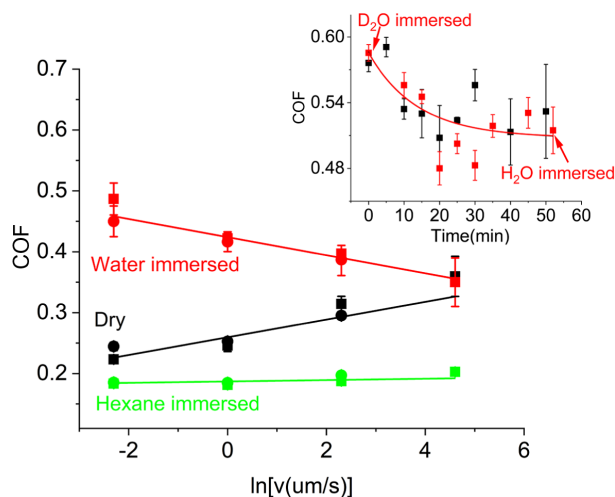


FIG. 3. Dependence of the friction coefficient on sliding velocity. The red, black, and green data correspond to the friction coefficient measured at increasing (squares) and decreasing (solid circles) velocities ranging from 0.1 to 100  $\mu\text{m/s}$  in the dry case (relative humidity = 0.6%), the water-immersed case, and hexane-immersed case, respectively. The inset displays the change in friction coefficient as a function of time, measured as the  $\text{D}_2\text{O}$  immersed contact evolves into an  $\text{H}_2\text{O}$  immersed contact. In the inset, the red and black colored data points (squares) correspond to two independent experiments.

attraction between sand grains by increasing capillary pressure, while too much water causes the merging of water bridges, destabilizing the sand finally. Similar non-monotonic friction trends, but with different mechanisms, have been explored at the carbon and graphite contact interface, where the nonmonotonic change is dominated by contact quality or the number of pinning sites of intercalated water molecules [9]. For Si-on-Si multiasperity friction at high relative humidities here, the reduction in Laplace pressure leads to the decrease in capillary adhesion and, thus, in friction coefficient. It should be noted that the precise dependence of the friction coefficient on relative humidity depends on the interface topography. The detailed estimates of capillary adhesive forces in various relative humidities are listed in Table S2.

Despite the good agreement between measured and predicted COF at high relative humidities ( $> 20\%$ ), our adhesion model fails to predict the dramatic drop in friction coefficient observed at low ( $< 20\%$ ) relative humidities. Also, the substantial difference in friction between the dry measurement and the water-immersed measurement has not been observed previously in single asperity experiments [33,34]. Capillary adhesion cannot explain this difference in friction since there is no capillary adhesion in either the dry or water-immersed environments. Furthermore, hydrodynamic lubrication can be excluded since the sliding system runs in the boundary lubrication regime considering the low sliding speed (0.1  $\mu\text{m/s}$ ) and high contact pressure

(3 GPa) in combination with the low viscosity of water ( $1.0 \times 10^{-3}$  Pa s at 20  $^\circ\text{C}$ ).

We propose that the difference in friction measured at 0.6% RH and in the water-immersed condition originates from physical or covalent interfacial bonding associated with the presence of water [35–37]. That this is specific to water follows from a reference experiment performed in hexane vapor, where, in fact, the 1% RH friction is lowered by the addition of hexane vapor, and the strong asymmetry between the friction measured in hexane vapor and hexane immersion is absent (Fig. 2). This suggests that hydrogen bonding may play an important role whenever water is present. To test this hypothesis further, we repeat the experiments using heavy water ( $\text{D}_2\text{O}$ ) instead of water, the former having significantly stronger hydrogen bonds [38,39]. We therefore carry out an immersed friction experiment using heavy water, and indeed find that the friction is  $14 \pm 5\%$  higher. This increase cannot be due to the higher viscosity of  $\text{D}_2\text{O}$ , since the viscous contribution to the friction is negligible at the velocities used in our experiments (see previous paragraph). To demonstrate that the higher friction of the heavy-water immersed contact is not due to experimental variability, we use the fact that  $\text{D}_2\text{O}$  exchanges easily with  $\text{H}_2\text{O}$  from humid air. We therefore repeat the experiment starting with a  $\text{D}_2\text{O}$  lubricated contact and introducing  $\text{H}_2\text{O}$ -humid air into the experimental chamber.

As shown in the inset of Fig. 3, the friction coefficient gradually decreases from  $\mu = 0.58$  to  $\mu = 0.51$  as  $\text{D}_2\text{O}$  exchanges with  $\text{H}_2\text{O}$  from the surrounding air in two subsequent experiments. Similar rapid H/D exchange has been described in hydroxyl accessibility studies of deuterated wood [40]. The higher friction at the heavy water-immersed interface can be attributed to the stronger hydrogen bonding compared with  $\text{H}_2\text{O}$  [38,39,41]. As heavy water at the interface is gradually replaced by normal water from the humid environment, the friction decreases due to the weaker interfacial hydrogen bond network. The interplay between the hydrogen bond network and adhesion has previously been demonstrated in AFM studies on silica through manipulating the solvent pH [42,43].

The assumption that the hydrogen bonding contributes to the friction is also supported by our velocity-dependent experiments, as shown in Fig. 3. An approximately linear increase in friction with the logarithm of the sliding velocity is observed in the velocity range from 0.1 to 100  $\mu\text{m/s}$  in the dry environment (0.6% RH). The velocity strengthening of the dry friction is commonly attributed to thermally activated slip in which the shear stress lowers the activation barrier [44]. A spectacular observation is that the friction of the fully immersed contact shows a decreasing COF with increasing velocity, exactly the opposite of the dry friction. As explained before, viscous

effects such as hydrodynamic lubrication cannot take place at such low sliding velocities and high contact pressures. It is tempting to attribute the velocity-weakening friction to the dynamic equilibrium between the rupture and formation of the hydrogen-bonding network at the interface [45]. As the velocity increases, the rate at which interfacial hydrogen bonds are broken outpaces the rate at which interfacial hydrogen bonds are formed, thus leading to a smaller friction force. We can, very roughly, quantify this idea as follows. Given the typical length and formation time of a hydrogen bond in water (order of magnitude 1 nm and 1 ps, respectively) [46], we expect that at velocities above order  $10^3$  m/s, H-bond formation should no longer contribute significantly to the friction. This expectation is indeed supported by the extrapolated velocity dependence in water-immersed friction measurements, in which the friction is predicted to be as low as  $0.11 \pm 0.05$  at a velocity of  $10^3$  m/s. Indeed this is comparable to the velocity-independent friction measured under hexane-immersed conditions, further corroborating our interpretation, as there would be no interfacial hydrogen bonding facilitated by the alkane.

In conclusion, we have investigated the evolution of capillary adhesion and friction with relative humidity in a multiasperity Si-on-Si system: the coefficient of friction first increases sharply in the relative humidity range from 0 to 20%, and then decreases slightly with increasing relative humidity at humidities above 20%. This evolution of the coefficient of friction with relative humidity can be influenced by drying hysteresis. To understand the change in the coefficient of friction, an adhesion model based on the boundary element method is employed and shown to capture the dependence of the coefficient of friction on relative humidity at humidities above 20%. The reduction in friction with increasing relative humidity originates from the decrease in capillary adhesion with increasing relative humidity due to the drop in Laplace pressure. The strong decrease in friction with decreasing relative humidity in the low relative humidity regime is attributed to the lack of capillary adhesion and the reduced effect of interfacial bonding by the hydrogen-bond network of water between the interfaces, as evidenced by the velocity-dependent friction experiments. Our results indicate that interfacial hydrogen bonding during sliding contributes to friction.

This Letter is part of the project Friction on demand: to slide or not to slide with Project No. VI.Veni.192.177, which is (partly) financed by the Dutch Research Council. We are grateful for financial support from the MaxWater Initiative of the Max Planck Society. We thank Dr. Chen Xiao and Dr. Felix Cassin for discussions and AFM measurements. Liang Peng acknowledges funding from China Scholarship Council and encouragement from Prof. Bingsuo Pan and Dr. Songcheng Tan.

\*Corresponding author.

l.peng@uva.nl

- [1] A. L. Barnette, J. A. Ohlhausen, M. T. Dugger, and S. H. Kim, Humidity effects on *in situ* vapor phase lubrication with n-pentanol, *Tribol. Lett.* **55**, 177 (2014).
- [2] M. Scherge, X. Li, and J. Schaefer, The effect of water on friction of mems, *Tribol. Lett.* **6**, 215 (1999).
- [3] L. Chen, C. Xiao, B. Yu, S. H. Kim, and L. Qian, What governs friction of silicon oxide in humid environment: Contact area between solids, water meniscus around the contact, or water layer structure?, *Langmuir* **33**, 9673 (2017).
- [4] F.-C. Hsia, S. Franklin, P. Audebert, A. M. Brouwer, D. Bonn, and B. Weber, Rougher is More Slippery: How Adhesive Friction Decreases with Increasing Surface Roughness Due to the Suppression of Capillary Adhesion, *Phys. Rev. Lett.* **3**, 043204 (2021).
- [5] F.-C. Hsia, C.-C. Hsu, L. Peng, F. M. Elam, C. Xiao, S. Franklin, D. Bonn, and B. Weber, Contribution of Capillary Adhesion to Friction at Macroscopic Solid–Solid Interfaces, *Phys. Rev. Appl.* **17**, 034034 (2022).
- [6] D. B. Asay and S. H. Kim, Effects of adsorbed water layer structure on adhesion force of silicon oxide nanoasperity contact in humid ambient, *J. Chem. Phys.* **124**, 174712 (2006).
- [7] M. He, A. Szuchmacher Blum, D. E. Aston, C. Buenviaje, R. M. Overney, and R. Luginbühl, Critical phenomena of water bridges in nanoasperity contacts, *J. Chem. Phys.* **114**, 1355 (2001).
- [8] J. Seppä, B. Reischl, H. Sairanen, V. Korpelainen, H. Husu, M. Heinonen, P. Raiteri, A. L. Rohl, K. Nordlund, and A. Lassila, Atomic force microscope adhesion measurements and atomistic molecular dynamics simulations at different humidities, *Meas. Sci. Technol.* **28**, 034004 (2017).
- [9] K. Hasz, Z. Ye, A. Martini, and R. W. Carpick, Experiments and simulations of the humidity dependence of friction between nanoasperities and graphite: The role of interfacial contact quality, *Phys. Rev. Mater.* **2**, 126001 (2018).
- [10] D. Asay, M. De Boer, and S. Kim, Equilibrium vapor adsorption and capillary force: Exact laplace–young equation solution and circular approximation approaches, *J. Adhes. Sci. Technol.* **24**, 2363 (2010).
- [11] M. Farschi-Tabrizia, M. Kappl, and H.-J. Butt, Influence of humidity on adhesion: An atomic force microscope study, *J. Adhes. Sci. Technol.* **22**, 181 (2008).
- [12] L. Chen and L. Qian, Role of interfacial water in adhesion, friction, and wear—a critical review, *Friction and wear in machinery* **9**, 1 (2021).
- [13] M. Pakpour, M. Habibi, P. Møller, and D. Bonn, How to construct the perfect sandcastle, *Sci. Rep.* **2**, 549 (2012).
- [14] A. Fall, B. Weber, M. Pakpour, N. Lenoir, N. Shahidzadeh, J. Fiscina, C. Wagner, and D. Bonn, Sliding Friction on Wet and Dry Sand, *Phys. Rev. Lett.* **112**, 175502 (2014).
- [15] P. C. Møller and D. Bonn, The shear modulus of wet granular matter, *Europhys. Lett.* **80**, 38002 (2007).
- [16] E. Riedo, F. Lévy, and H. Brune, Kinetics of Capillary Condensation in Nanoscopic Sliding Friction, *Phys. Rev. Lett.* **88**, 185505 (2002).
- [17] M. Bazrafshan, M. de Rooij, and D. Schipper, Adhesive force model at a rough interface in the presence of thin water

- films: The role of relative humidity, *Int. J. Mech. Sci.* **140**, 471 (2018).
- [18] O. Noel, P.-E. Mazeran, and H. Nasrallah, Sliding Velocity Dependence of Adhesion in a Nanometer-Sized Contact, *Phys. Rev. Lett.* **108**, 015503 (2012).
- [19] F. W. DelRio, M. L. Dunn, L. M. Phinney, C. J. Bourdon, and M. P. de Boer, Rough surface adhesion in the presence of capillary condensation, *Appl. Phys. Lett.* **90**, 163104 (2007).
- [20] E. Soylemez and M. P. De Boer, Modeling capillary bridge dynamics and crack healing between surfaces of nanoscale roughness, *J. Micromech. Microeng.* **27**, 125023 (2017).
- [21] L. A. Thimons, A. Gujrati, A. Sanner, L. Pastewka, and T. D. Jacobs, Hard-material adhesion: Which scales of roughness matter?, *Exp. Mech.* **61**, 1109 (2021).
- [22] B. N. Persson, O. Albohr, U. Tartaglino, A. Volokitin, and E. Tosatti, On the nature of surface roughness with application to contact mechanics, sealing, rubber friction and adhesion, *J. Phys. Condens. Matter* **17**, R1 (2005).
- [23] A. Tiwari, J. Wang, and B. N. J. Persson, Adhesion paradox: Why adhesion is usually not observed for macroscopic solids, *Phys. Rev. E* **102**, 042803 (2020).
- [24] C. Leriche, S. Franklin, and B. Weber, Measuring multi-asperity wear with nanoscale precision, *Wear* **498**, 204284 (2022).
- [25] F.-C. Hsia, F. M. Elam, D. Bonn, B. Weber, and S. E. Franklin, Wear particle dynamics drive the difference between repeated and non-repeated reciprocated sliding, *Tribol. Int.* **142**, 105983 (2020).
- [26] See Supplemental Material at <http://link.aps.org/supplemental/10.1103/PhysRevLett.129.256101> for experimental result of friction hysteresis as a function of relative humidity, direct measurement of multi-asperity adhesion, additional result of the friction measurement and simulation as a function of relative humidity, basic parameters for contact simulation.
- [27] Available at: <https://www.tribonet.org/cmdownloads/tribosolver-2/>.
- [28] S. Kim, D. Kim, J. Kim, S. An, and W. Jhe, Direct Evidence for Curvature-Dependent Surface Tension in Capillary Condensation: Kelvin Equation at Molecular Scale, *Phys. Rev. X* **8**, 041046 (2018).
- [29] C. Xiao, C. Chen, Y. Yao, H. Liu, L. Chen, L. Qian, and S. H. Kim, Nanoasperity adhesion of the silicon surface in humid air: The roles of surface chemistry and oxidized layer structures, *Langmuir* **36**, 5483 (2020).
- [30] A. Berman, C. Drummond, and J. Israelachvili, Amontons' law at the molecular level, *Tribol. Lett.* **4**, 95 (1998).
- [31] J. Israelachvili, S. Giasson, T. Kuhl, C. Drummond, A. Berman, G. Luengo, J.-M. Pan, M. Heuberger, W. Ducker, and N. Alcantar, Some fundamental differences in the adhesion and friction of rough versus smooth surfaces, *Tribol. Series* **38**, 3 (2000).
- [32] X. He, Z. Liu, L. B. Ripley, V. L. Swensen, I. J. Griffin-Wiesner, B. R. Gulner, G. R. McAndrews, R. J. Wieser, B. P. Borovsky, Q. J. Wang *et al.*, Empirical relationship between interfacial shear stress and contact pressure in micro-and macro-scale friction, *Tribol. Int.* **155**, 106780 (2021).
- [33] C. Chen, C. Xiao, X. Wang, P. Zhang, L. Chen, Y. Qi, and L. Qian, Role of water in the tribochemical removal of bare silicon, *Appl. Surf. Sci.* **390**, 696 (2016).
- [34] X. Wang, S. H. Kim, C. Chen, L. Chen, H. He, and L. Qian, Humidity dependence of tribochemical wear of mono-crystalline silicon, *ACS Appl. Mater. Interfaces* **7**, 14785 (2015).
- [35] Q.-Y. Tong, T.-H. Lee, U. Gösele, M. Reiche, J. Ramm, and E. Beck, The role of surface chemistry in bonding of standard silicon wafers, *J. Electrochem. Soc.* **144**, 384 (1997).
- [36] T. Plach, K. Hingerl, S. Tollabimazraehno, G. Hesser, V. Dragoi, and M. Wimplinger, Mechanisms for room temperature direct wafer bonding, *J. Appl. Phys.* **113**, 094905 (2013).
- [37] J. Yu, S. H. Kim, B. Yu, L. Qian, and Z. Zhou, Role of tribochemistry in nanowear of single-crystalline silicon, *ACS Appl. Mater. Interfaces* **4**, 1585 (2012).
- [38] S. Scheiner and M. Čuma, Relative stability of hydrogen and deuterium bonds, *J. Am. Chem. Soc.* **118**, 1511 (1996).
- [39] H. Schott, Direct comparison of the strength of hydrogen bonds formed by H<sub>2</sub>O and D<sub>2</sub>O, *J. Macromol. Sci. Part B* **27**, 119 (1988).
- [40] A. Tarmian, I. Burgert, and E. E. Thybring, Hydroxyl accessibility in wood by deuterium exchange and ATR-FTIR spectroscopy: Methodological uncertainties, *Wood science and technology* **51**, 845 (2017).
- [41] G. Nemethy and H. A. Scheraga, Structure of water and hydrophobic bonding in proteins. IV. The thermodynamic properties of liquid deuterium oxide, *J. Chem. Phys.* **41**, 680 (1964).
- [42] J. D. Batteas, X. Quan, and M. K. Weldon, Adhesion and wear of colloidal silica probed by force microscopy, *Tribol. Lett.* **7**, 121 (1999).
- [43] J. D. Batteas, M. K. Weldon, and K. Raghavachari, Bonding and interparticle interactions of silica nanoparticles, in *Nanotribology* (Springer, New York, 2003), pp. 387–398.
- [44] Y. Bar-Sinai, R. Spatschek, E. A. Brener, and E. Bouchbinder, On the velocity-strengthening behavior of dry friction, *J. Geophys. Res.* **119**, 1738 (2014).
- [45] J. Chen, I. Ratera, J. Y. Park, and M. Salmeron, Velocity Dependence of Friction and Hydrogen Bonding Effects, *Phys. Rev. Lett.* **96**, 236102 (2006).
- [46] R. A. Nicodemus, S. Corcelli, J. Skinner, and A. Tokmakoff, Collective hydrogen bond reorganization in water studied with temperature-dependent ultrafast infrared spectroscopy, *J. Phys. Chem. B* **115**, 5604 (2011).